Environmental Science & Technology

Article

pubs.acs.org/est

Probing the Evaporation Dynamics of Mixed SOA/Squalane Particles Using Size-Resolved Composition and Single-Particle Measurements

Ellis Shipley Robinson, Rawad Saleh, and Neil M. Donahue*

Center for Atmospheric Particle Studies, Carnegie Mellon University, 5000 Forbes Avenue, Pittsburgh, Pennsylvania 15213, United States

Supporting Information

ABSTRACT: An analysis of the formation and evaporation of mixed-particles containing squalane (a surrogate for hydrophobic primary organic aerosol, POA) and secondary organic aerosol (SOA) is presented. In these experiments, one material (D_{62}-squalane or SOA from α-pinene + O_3) was prepared first to serve as surface area for condensation of the other, forming the mixed-particles. The mixed-particles were then subjected to a heating-ramp from 22 to 44 °C. We were able to determine that (1) almost all of the SOA mass is comprised of material less volatile than D_{62}-squalane; (2) AMS collection efficiency in these mixed-particle systems can be parametrized as a function of the relative mass fraction of the components; and (3) the vast majority of D_{62}-squalane is able to evaporate from the mixed particles, and does so on the same time scale regardless of the order of preparation. We also performed two-population mixing experiments to directly test whether D_{62}-squalane and SOA from α-pinene + O_3 form a single solution or two separate phases. We find that these two OA types are immiscible, which informs our inference of the morphology of the mixed-particles. If the morphology is core−shell and dictated by the order of preparation, these data indicate that squalane is able to diffuse relatively quickly through the SOA shell, implying that there are no major diffusion limitations.

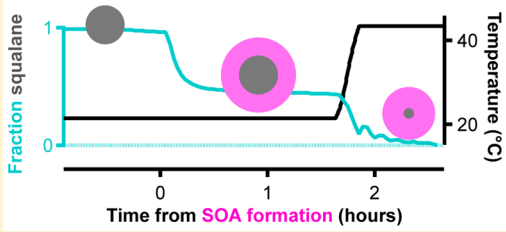

INTRODUCTION

Atmospheric aerosol particles negatively influence human health and also have a large, yet highly uncertain effect on the climate.[1] The organic fraction of atmospheric particulate matter (PM) comprises 20−90% of the submicron PM mass, and is a complex mixture of myriad species emitted either directly as particles (primary organic aerosol (POA)) or transferred to the condensed phase through oxidative chemistry (secondary organic aerosol (SOA)).[2] Owing largely to this chemical complexity, the processes surrounding the formation, growth, and chemical evolution of OA in the atmosphere are not fully understood, as evinced by a persistent gap between measured atmospheric OA and the predictions of regional chemical transport models.[3]

Many predictive models assume that all classes of OA (e.g., biogenic SOA, hydrophobic POA) form a single, pseudoideal condensed phase.[4] This requires that all OA types are miscible and exhibit no barriers to mass transfer that would cause the mixing process to play out over multiple timesteps within models. This also requires that equilibration with a changing gas-phase happens on time scales shorter than the model timesteps. It has been recently proposed that these assumptions may not hold under certain circumstances for many types of OA, and that this may significantly contribute to the discrepancy between models and measurements.[5−7]

First, theoretical considerations support the presence of a nonpolar "organic" phase containing most POA and a polar "aqueous" phase containing most SOA.[8] Multiple recent smog chamber studies present convincing evidence for phase-separation between different classes of OA (e.g., different varieties of SOA and POA, as in Song et al.,[9] Asa-Awuku et al.,[10] and Robinson et al.[11]). Very probably there are multiple condensed organic phases present in the atmospheric OA ensemble, especially in urban areas with diverse sources of particles. Second, recent experimental studies indicate that SOA can evaporate slowly; consistent with slow equilibration. Vaden et al.[12] reported evaporation rates of SOA in a vapor-free environment that were much slower than predicted based on previously reported volatility distributions. These data were used to conclude that there are diffusion limitations to mass transfer within the particle bulk. Perraud et al.[13] reported differences between measured particle-phase concentrations of organic nitrates in SOA and their expected concentrations assuming ideality, implicating either variable activity coefficients as a function of OA concentrations for organic nitrates in SOA, or mass transfer limitations. In evaporation studies using pyrene as a chemical tracer for diffusion within SOA, Abramson et al.[5] and Zelenyuk et al.[14] both reported evaporation rates for trace levels of pyrene embedded in SOA slower than for pure pyrene, also arguing that molecular diffusion of organics within SOA is very slow.

Simultaneously, recent work[15,16] shows that some SOA components are probably much less volatile than previous

Received: April 3, 2015
Revised: June 26, 2015
Accepted: July 9, 2015
Published: July 9, 2015

ACS Publications © 2015 American Chemical Society

DOI: 10.1021/acs.est.5b01692
Environ. Sci. Technol. 2015, 49, 9724−9732

studies had suggested.[17] A much lower volatility for SOA would potentially explain (as suggested by Saleh et al.[18]) the slow evaporation seen in the aforementioned studies, without invoking mass transfer limitations. Similarly, nonmixing between different types of OA has recently been cited as evidence for slow diffusivity within SOA,[19] though low volatility and/or miscibility limitations could potentially explain such data as well. In general, a thorough understanding of a given system's expected phase behavior and volatility distribution(s) are required to draw firm conclusions about mass transfer within particles, and all of these aspects are important for how OA dynamics are conceptualized in chemical transport models.

The experiments presented here probe mixing, mass transfer, and volatility of SOA. We present experiments in which particles composed of two demonstrably immiscible phases—D_{62}-squalane and SOA—are sequentially prepared (e.g., SOA is formed and condensed onto squalane seeds, and vice versa), and then subjected to a temperature elevation ramp. Contingent on the morphology of these mixed-particles (e.g., an SOA shell on a squalane core), these experiments provide a direct test of organic diffusivity within SOA during the temperature-ramp perturbation. We present evaporation results for these mixed-particles, and estimate the fraction of the SOA with volatility lower than that of squalane.

■ MATERIALS AND METHODS

We performed variations on two basic experiments: (1) separately preparing two aerosol populations and combining them into a common volume, and (2) preparing mixed-particles of uniform (nominally core−shell) composition. All experiments were conducted in dry smog chamber conditions (RH < 5%). Both experimental procedures and the measurement suite used are detailed in the following section.

Two-Population Experiments. We have reported the concept and procedure for two-population experiments in detail previously.[11] In brief, two aerosol populations are prepared in separate chambers, and then combined into a shared volume. By using single-particle mass spectrometry, we can track the composition of each population and attribute further compositional changes to mixing. Despite recent advances in methods to collect SOA for bulk analysis (e.g., Renbaum-Wolff et al.[20]), which could be useful for studying phase behavior (mixing) between SOA and other OA types of interest, we believe that these two-population experiments provide unique insight into the miscibility between different types of OA, as the particle size and composition is truer to that found in the atmosphere (e.g., extracting the water-soluble components of SOA from filters and resuspending it may change its properties). Here the purpose of these two-population experiments is to determine whether squalane and the α-pinene SOA are miscible.

In this mixing experiment, we prepared SOA from the reaction of α-pinene + O_3 in a 50 L sample bag. The bag was charged with excess ozone, into which 1.2 μL of α-pinene (Sigma-Aldrich, >99%) was injected through a heated tube fitted with an airtight septum (assuming all of the precursor is transferred to the bag, the mixing ratio of α-pinene is 3.7 ppm). After 15 min, the contents of the sample bag were then diluted by a factor of ∼200 into a 10 m^3 smog chamber, and left for 1 h for characterization. The reason for preparing the SOA this way, as opposed to in the smog chamber directly, was to ensure that particles were large enough to be measured by the light-scattering single-particle (LSSP) module of the AMS, which has a lower optical detection limit of d_{va} = 180 nm. It should be noted that the SOA in these experiments was formed at high concentration (mass yield curves suggest $C_{OA} \sim 6$ mg m^{-3}) but then diluted to a much lower value ($C_{OA} \sim 30$ μg m^{-3}). In a separate 50 L sample bag, we prepared D_{62}-squalane particles (C/D/N Isotopes, 99%) by flash vaporization. An aliquot of 0.8 μL of D_{62}-squalane was placed onto the tip of a stainless-steel heater, which was then inserted into the sample bag for in situ vaporization. Homogeneously nucleated D_{62}-squalane particles formed immediately. The contents of this bag were also then diluted into the larger smog chamber, already containing SOA. This experiment was performed to establish whether or not SOA and D_{62}-squalane mix together to form a single phase or remain phase-separated.

At the time of the addition of the squalane population to the chamber, the measured condensation sink of the SOA was CS = 0.33 min^{-1} (the squalane population had a similar value), compared to a value of 0.1 min^{-1} that we calculate for the walls of the smog chamber. So while there may be vapors from either population lost to the walls (as has been noted previously for organic aerosol Teflon chamber experiments, for example, Matsunaga and Ziemann[21]), the mixing time scale is faster than the vapor wall loss time scale, so if mixing is thermodynamically favorable it should be observed here.

Mixed-Particle Experiments. We performed two types of mixed-particle experiments: (1) SOA particles were used as seeds for condensation of D_{62}-squalane, and (2) D_{62}-squalane particles were used as seeds for condensation of SOA. In all cases, the SOA was formed from the reaction of α-pinene + O_3.

For experiments using D_{62}-squalane as seed particles, D_{62}-squalane was flash vaporized, as described above, directly into the 10 m^3 Teflon smog chamber. High heat and low (3 lpm) flow of dispersal air was used to ensure a high supersaturation in the vapor plume which led to large particles (number mode diameter, d = 160 nm; condensation sink, CS = 0.34 min^{-1}). After formation and characterization of the D_{62}-squalane particles, the smog chamber was charged with ozone (∼1−2 ppm), and then a 1.2 μL aliquot of α-pinene was injected into the chamber through a heated tube fitted with a septum (assuming perfect transmission of α-pinene to the chamber, the mixing ratio would be 20 ppb). Clean, dry air was used to carry α-pinene vapor into the smog chamber, after which it reacted with O_3 to form SOA that condensed on the squalane seeds.

In the reverse experiment, where SOA was used as seed particles for condensation of D_{62}-squalane, SOA was formed under the same conditions described in the previous section (SOA from 1.2 μL α-pinene + excess O_3 was prepared in and then diluted from a 50 L sample bag into the 10 m^3 smog chamber). Following SOA characterization in the 10 m^3 smog chamber, D_{62}-squalane was vaporized directly into the chamber after which it condensed onto the SOA particles. The flash vaporization was conducted with low-heat and a high (15 lpm) flow of dispersal air, to dilute the high-concentration D_{62}-squalane plume as much as possible. This reduced the supersaturation of the squalane, preventing any new particle formation.

After preparation and characterization of the mixed-particles, the smog chamber temperature was elevated from 22 to 44 °C, perturbing the equilibrium of the system, and prompting evaporation.

Instrument Suite. Relative humidity and temperature in the smog chamber were monitored using a commercial humidity monitor (Vaisala, HNP-233). Ozone was generated

DOI: 10.1021/acs.est.5b01692
Environ. Sci. Technol. 2015, 49, 9724−9732

by flowing oxygen through a corona-discharge ozone generator (Azco, HTU500AC) and measured using a UV photometric ozone monitor (Dasibi, 1008-PC). Ensemble particle volume and number concentrations were measured using an SMPS (SMPS; TSI, Inc.).

OA composition and mass were measured with a high-resolution aerosol mass spectrometer (HR-Tof-AMS; Aerodyne, Inc.) operated in single-reflectron V-mode, fully described by DeCarlo et al.[22] Data were collected in mass spectrometer (MS) mode (providing bulk aerosol composition) and particle time-of-flight (PToF) mode (providing aerosol chemical composition as a function of vacuum aerodynamic diameter, d_{va}), and analyzed using custom software packages SQUIRREL (v1.51A) and PIKA (v1.12C). Mass spectra from individual particles were acquired using a light-scattering single-particle (LSSP) module coupled to the HR-ToF-AMS,[23] and analyzed using the SPARROW (v1.04A) software package (all software packages mentioned above were written by Donna Sueper of Aerodyne Research Inc./CU-Boulder, and can be accessed at http://cires1.colorado.edu/jimenez-group/ToFAMSResources/ToFSoftware/index.html).

Briefly, LSSP data consists of light-scattering and mass spectral signals from individual particles. LSSP data provide an in situ measurement of collection efficiency (CE) in the AMS, as some particles that enter the flight-chamber of the instrument (and thus scatter light) are undetected by the mass spectrometer. Particles can be lost at various stages in the instrument, including the aerodynamic lens and the particle flight chamber, but most often, including this study, CE is governed largely by the propensity for a particle type to bounce (or not) from the AMS vaporizer before it is able to vaporize,[24] thus avoiding ionization and detection. For a more complete discussion of AMS CE, see Huffman et al.[25] We used an operationally defined threshold of 6 ions to distinguish null particle events from particles giving meaningful chemical mass signals (as in Liu et al.[26]). CE was calculated according to the following equation:

$$\mathrm{CE} = \frac{\text{particles with MS signal} > 6\text{ ions}}{\text{particles with LS signal}} \quad (1)$$

Both "prompt" and "delayed" particles can contribute signals above this threshold. The distinction between these two categories is that delayed signals arrive at the mass detector ($\mathrm{MS_{arrival}}$) much later than is predicted ($\mathrm{LS_{arrival}}$) based on the velocity as measured by optical scattering. The distinction between prompt and delayed particles is an arbitrarily imposed threshold where delayed particles take at least 20% longer to arrive than is expected ($\mathrm{MS_{arrival}}/\mathrm{LS_{arrival}} > 1.2$).

RESULTS

Two-Population Mixing of SOA and Squalane. Previously, we have shown that squalane OA is volatile enough to mix through gas-phase exchange on the time scales of smog chamber experiments, by conducting a two-population experiment with isotopically labeled/unlabeled squalane.[11] We also showed that D_{62}-squalane OA and SOA formed from toluene oxidation do not mix together, despite the lack of a diffusive barrier to absorption of toluene-SOA vapors into liquid squalane particles, and the availability of semivolatile squalane vapors that could partition into the toluene-SOA mass. The reason for the lack of mixing is simply that thermodynamics does not favor it—like oil and water, squalane and SOA from toluene oxidation are immiscible.

Extending this previous work, here we present results from a two-population experiment using D_{62}-squalane particles and SOA particles from α-pinene ozonolysis, shown in Figure 1. We

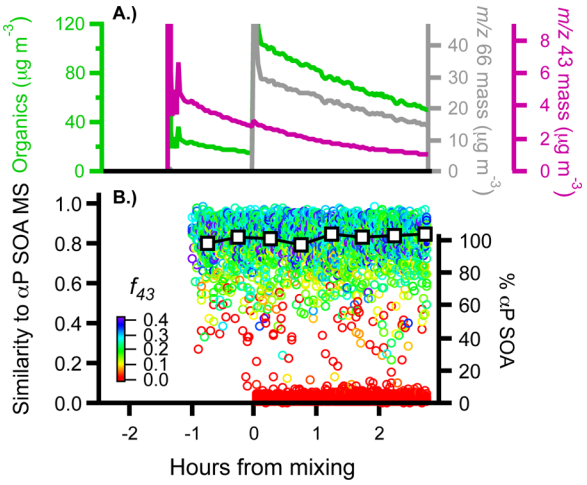

Figure 1. Time series of a two-population experiment demonstrating that SOA from α-pinene + O_3 and squalane OA do not mix. (A.) In top panel, total organic mass (left axis) and unique tracer fragments (m/z 43 for SOA and m/z 66 for D_{62}-squalane, right axes) are plotted. Prior to $t = 0$, only SOA is present in the chamber. At $t = 0$, D_{62}-squalane particles are added to the chamber (marked by m/z 66). (B.) Bottom panel shows the uncentered correlation coefficients, a metric of mass spectral similarity to a reference, for all prompt particles (left axis). SOA is used as the reference MS. Data points are colored by the fraction of m/z 43 in each particle. The black squares in the bottom panel show the % α-pinene SOA (right axis) in the originally-SOA population as calculated using the single-particle data.

see the persistence of two chemically distinct aerosol populations over the course of ~2 h after the particle populations are combined, with no sign of convergence, indicative of nonmixing. The time series in the top panel shows the total organic mass (green), and mass spectral fragments highly specific to each particle type (m/z 66, entirely comprised of $C_4D_9^+$ for D_{62}-squalane and m/z 43, largely $C_2H_3O^+$, for SOA). The mass concentrations in the top panel decrease due to particle losses to walls. The bottom panel shows the uncentered correlation coefficients of individual particles, a common measure of similarity between a mass spectrum and some reference spectrum[27] (in this case, the reference is the average mass spectrum (MS) for SOA from LSSP-mode). Values close to one signify a single-particle MS is similar to the reference while values close to zero mean the MS is dissimilar to the reference. Data points are colored by the fraction of m/z 43 ("f_{43}") to the total signal in each particle MS. The distribution of f_{43} is centered at 0.2. This agrees well with the bulk measurement, though there is a wide distribution of values measured because of the relatively low number of ions measured from each individual particle. At $t = 0$ h, D_{62}-squalane particles are added to the SOA-filled chamber (shown by the gray trace in top panel, and red circles in lower panel). Were squalane particles absorbing vapors from the SOA, we would see m/z 43 in their mass spectra and an increase in their similarity to the reference, neither of which are evident. Additionally, we see no absorption of m/z 66 into the SOA

DOI: 10.1021/acs.est.5b01692
Environ. Sci. Technol. 2015, 49, 9724−9732

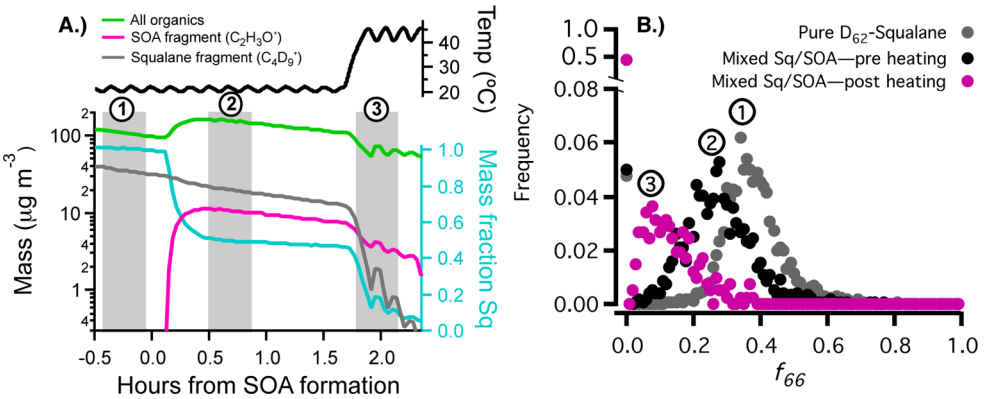

Figure 2. (A) Time series of a mixed-particle experiment where D_{62}-Squalane particles served as seeds for the condensation of SOA from α-pinene ozonolysis, followed by a heating ramp. This plot illustrates the ability of squalane to evaporate from these mixed particles. AMS signals from MS-mode are shown on the left y-axis versus time from SOA formation: $C_4H_9^+$ (fragment unique to D_{62}-squalane, gray), $C_4H_3O^+$ (fragment unique to SOA, pink), and total organics (green). Mass-fraction of squalane to the total OA is shown on the right y-axis (teal). At $t \sim 1.5$ h the chamber temperature is ramped from 22 to 44 °C. Upon heating, the majority of the squalane mass evaporates, and the OA becomes almost entirely comprised of SOA, shown by mass fraction squalane going to zero. (B): Numbers 1−3 show time periods used for histograms of prompt, single-particle f_{66} values, where m/z 66 is entirely composed of $C_4H_9^+$, a tracer for D_{62}-squalane. The evolution of the three f_{66} histograms illustrates the inherent spread of single-particle MS even for pure compounds, the addition of SOA to the squalane seeds on a single-particle basis, and the significant evaporation of squalane (and enrichment in SOA) across all particles, respectively.

particles, which would dilute the amount of SOA mass in the SOA population, decreasing f_{43}.

In the experiment presented in Figure 1, the size-distributions for squalane and SOA are coincident (not shown)—they are almost completely overlapped in diameter space. The conclusions made by Asa-Awuku et al.[10] on the mixing between SOA and diesel-exhaust POA would not have been possible in such a case, as their analysis relied on the separation of unique marker fragments in diameter space to diagnose the initial populations as externally mixed. Using single-particle mass spectrometry, the only information required to determine whether OA populations mix or not is chemical composition in individual particles over the course of the experiment.

Coagulation is not expected to be a significant mechanism for mixing for the number concentration of these experiments ($N \approx 10\,000$ cm^{-3}). We calculate the time scale for the number of particles to be reduced to half of the initial value due to coagulation to be 105 h. Indeed, were coagulation driving mixing, we would see particles with mixed composition in Figure 1, which we do not.

From these single-particle data, we can conclude that there is no gas-phase exchange between the particle populations, which rules out the possibility that squalane and SOA would be well-mixed even if present within single aerosol particles, as in the mixed-particle experiments. This result is expected, and agrees with the previous results of Vaden et al. that indicated phase separation in internally mixed SOA/dioctyl phthalate (DOP) particles[12] and our own results for squalane and toluene-derived SOA.[11] Like squalane, DOP is used as a surrogate for hydrophobic POA in smog chamber experiments. Because we are confident that squalane and the α-pinene SOA are immiscible, we can conclude that when we coat one type with the other, the resulting particles will adopt a phase-separated morphology. These experiments were conducted at low (>5%) RH, but are expected to hold for the range of atmospheric RH given that squalane is completely unoxidized and will not favor mixing with an oxidized/aqueous phase.

Evaporation Dynamics of Mixed SOA/Squalane Particles. We performed mixed-particle experiments, where one constituent (D_{62}-squalane or SOA) served as a surface for condensable vapors of the other constituent, after which the mixture was heated. The following analysis is shown for a representative experiment, but applies for other experiments, which are shown in the Supporting Information. Figure 2a shows a time-series for an experiment where D_{62}-squalane particles served as seeds for SOA formation. Like Figure 1, we use the same color scheme: gray corresponds to the D_{62}-squalane fragment ($C_4D_9^+$) and pink corresponds to the SOA fragment ($C_2H_3O^+$), which are plotted on the left y-axis (log scale). There were no new particles formed during the SOA chemistry, so all of the secondary organic matter (SOM) condensed onto the pre-existing squalane seeds. On the right axis, we plot the mass fraction of D_{62}-squalane to the total OA, which is calculated using following equation:

$$\text{mass fraction squalane} = \frac{f_{C_4D_9^+,t}}{f_{C_4D_9^+,t=0}} \tag{2}$$

where $f_{C4}D_9^+$ is defined as the ratio of $C_4D_9^+$ to total OA signal. This equation assumes that there is no chemistry ongoing in the chamber after SOA formation, and indeed we found no evidence of oxidized D_{62}-squalane fragments in the high-resolution MS. Upon formation of the SOM, the mass fractions of each component to the total OA are roughly equal in all mixed-particle experiments, though there is a mild decrease in the calculated mass fraction of squalane after SOA formation and prior to heating (3.5% decrease from $t = 0.6$ to 1.6 h). We attribute this to vapor wall loss of squalane to the Teflon walls, as we find no evidence of oxidized squalane fragments that might result from unscavenged hydroxyl radicals (from the ozonolysis of alpha pinene) reacting heterogeneously with squalane.

At $t = 1.5$ h, we heated the smog chamber from 22 to 44 °C. There is a sharp decrease of $C_4D_9^+$ and a more mild decrease of $C_2H_3O^+$ (Figure 2). Neither of these traces are corrected for any changes in AMS CE occurring as particle composition

DOI: 10.1021/acs.est.5b01692
Environ. Sci. Technol. 2015, 49, 9724−9732

changes during the heat ramp, though the total organic signal has been corrected for CE changes. The mass fraction of squalane in the total suspended aerosol decreases from 0.5 to 0.05. This indicates that (1) squalane is clearly evaporating from the mixed-particles, as 90% of the squalane is gone after heating, and that (2) squalane is more volatile than a significant fraction of the SOA. Squalane has a saturation concentration (C^{sat}) of approximately 8×10^{-2} μg m^{-3} at 22 °C (estimated using SIMPOL[28]). For this experiment, we calculate that there is very little evaporation of SOA (see Figure 4), meaning that almost all of the SOA mass is less volatile than squalane. We base this on the mass fraction remaining (MFR) of SOA after heating compared to the MFR of squalane after heating. There are further details in the following section about calculating the MFR of SOA.

Figure 2b illustrates how the single-particle mass spectra change before and after SOA formation, and after increasing the temperature of the smog chamber (averaging periods 1, 2, and 3, respectively, shown by shaded areas in Figure 2a). Here we see the inherent spread of single-particle mass signals: while the average value of the single-particle distribution for pure squalane (gray trace) agrees with the bulk measurement ($f_{66} \approx 0.4$), any given data point may fall within a wide range of measured f_{66}. This reflects the small number of ions detected from a single particle using electron impact ionization. After SOA is formed, and condensable products are added to the seed particles, the f_{66} distribution shifts to smaller values (black trace). The shift between the gray and black traces indicates that individual particles are indeed gaining SOA mass (squalane is "diluted" on a fractional basis of the total mass for a given particle). Again, given the results from the experiment shown in Figure 1, we expect these particles to contain two organic phases. Note that the number of particles with measured $f_{66} = 0$ is nonzero for pure D_{62}-squalane (averaging period 1), but does not increase with the addition of SOA (averaging period 2). An increase in the frequency of $f_{66} = 0$ events would serve as an indication of nucleation, but here the lack of such an increase further shows that the condensing SOA is condensing on the pre-existing seeds and forming particles with mixed-composition. After the chamber is heated, there is a further shift toward lower f_{66} values (averaging period 3). Many of the particles lose so much squalane that it is no longer measurable (note the appearance of a large number of $f_{66} = 0$ events on the split y-axis). Figure 2b shows that mixed squalane/SOA particles were formed, and that, upon heating, the squalane preferentially evaporates. This is fully consistent with the bulk measurements in Figure 2a, and more importantly verifies our data analysis on the basis of individual particles.

Because these mixed-phase particles are polydisperse and we expect two separate organic phases (SOA and squalane do not mix), the condensation of SOM should not be uniform across the distribution of squalane seeds—the amount of condensed SOM should instead be a function of size.[29] Condensational growth favors smaller particles with higher surface area-to-volume. Indeed, using mass distributions ($dM/d\log(d_{va})$) of the marker fragments from AMS PToF mode, we find that the mass fraction of squalane is lower (thus, SOA mass fraction is higher) for small particles. This is consistent with two phases being formed.[10,29] Figure 3 shows how the squalane mass fraction evolves for the three averaging periods as a function of particle size (top panel), along with the normalized PToF distributions for mass fragments specific to each material (middle and bottom panels). The PToF data are normalized

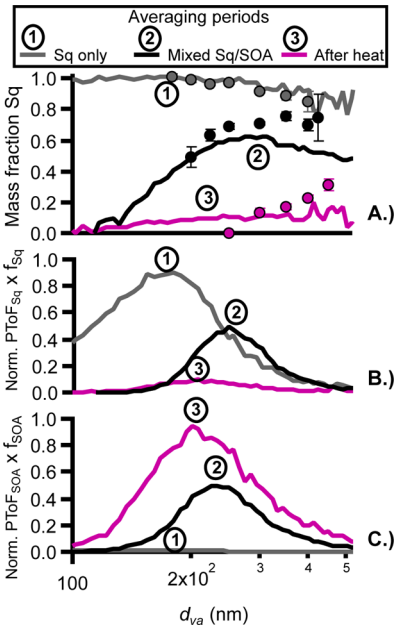

Figure 3. Size-resolved composition for the three averaging periods from Figure 2: D_{62}-squalane only (gray), post-SOA formation and condensation onto seed particles (black), and after heating the smog chamber (pink). These plots demonstrate the size-dependence of SOA condensation on the squalane seeds, and that squalane is evaporating across all sizes with heating. Top panel (A.) shows the mass fraction of D_{62}-squalane to the total OA versus size for all three intervals, as calculated from PToF-mode (lines) or single-particle-mode (circles) data. Middle (B.) and bottom (C.) panels show the evolution of the $dM/d\log d_{va}$ data (normalized by the value at the mode of the distribution) for marker fragments of D_{62}-squalane and SOA (m/z 66, middle, and m/z 43, bottom), both scaled by the overall mass fraction of each constituent.

here for display purposes: the mass distributions were scaled such that the value at the mode diameter matches the overall mass fraction of each material in a given averaging period (e.g., for the trace corresponding to mixed particles in the middle panel, the value at the mode has been scaled to be 0.5, matching the bulk mass fraction of squalane for that averaging interval).

Although it appears that there is a maximum in squalane mass fraction at roughly 300 nm for the mixed-particles, this is an artifact. Some types of OA do not promptly evaporate at the AMS vaporizer, which causes an artificial broadening of the mass distribution at large sizes (documented for ambient OA by Cross et al.[23]). This is true for the SOA in this study, which we conclude based on the mass spectra of delayed particles being enriched in SOA compared to squalane. Particles containing SOA do not vaporize as promptly as squalane, presumably because some bounce off of the vaporizer before ultimately vaporizing[30] due to differences in phase state between SOA and squalane (see "Collection Efficiency" section below). This makes large particles appear to contain more SOA than they actually do, as PToF data is calculated based on transit time from the chopper to the mass detector. Indeed, the squalane mass fraction as calculated from single-particle data has higher values than the PToF data for these large particle sizes, as shown in the top panel of Figure 3. Because single-particle size is optically determined (based on transit time between the chopper and laser), there is no artifact associated with delayed vaporization.

DOI: 10.1021/acs.est.5b01692
Environ. Sci. Technol. 2015, 49, 9724−9732

These data allow us to answer the following question: is squalane evaporating from particles across the size-range, or only for some particle sizes? Consider the following: perhaps the decrease in the bulk squalane mass fraction (teal trace, Figure 2a) largely is influenced by evaporation of the largest squalane particles, with the smallest relative amount of condensed SOA. The difference between the black and pink traces in the top panel of Figure 3 shows that this is not the case, and that squalane evaporates significantly across the entire size distribution. (For reference, if we assume a core−shell morphology, with SOA coating the squalane core, a 250 nm particle in this system has roughly a 30 nm thick SOA shell. See SI for plots of shell thickness vs size assuming core−shell.) These results are consistent with observations by Cappa and Wilson[31] of lubricating oil (LO) preferentially evaporating in a thermodenuder (residence time 15s) from mixed particles where SOA from α-pinene + O_3 had been condensed onto LO seeds. In their case, if we assume a core−shell morphology, the SOA shell would have been 15 nm thick for particles at the median of the particle number distribution.

When we prepare the mixed-particles in reverse order—SOA seed particles serving as condensational surface area for flash-vaporized squalane—we similarly see growth of particles to larger sizes and no nucleation, indicating that all squalane condensed onto the SOA seeds. Consistent with our earlier diagnosis of phase-separation within individual particles, we see a size-dependence to the mass fraction of squalane across particle size, with preferential condensation for the small end of the size spectrum[29] (in this case the squalane is more abundant on the smaller particles). Upon heating the smog chamber to 44 °C, we see significant evaporation of squalane across all particle sizes, with the bulk mass fraction of squalane decreasing from 0.75 to 0.1 before and after heating. The evaporation profile of squalane is qualitatively the same regardless of the order in which the mixed-particles are made (see Supporting Information Figure S1 for time series and mass fraction squalane as a function of size in this reverse experiment).

Collection Efficiency of Mixed SOA/Squalane Particles. We looked at particle collection efficiency as a potential probe for morphology in the mixed-particle experiments, as pure squalane and "pure" SOA particles are collected with different efficiencies in the AMS. Subunit CE for OA has been attributed to particles with a solid or semisolid phase state that have a greater likelihood to bounce off the AMS vaporizer surface before vaporization and subsequent ionization can occur, compared to liquid particles, which are collected with a near-unit CE.[32] Figure 4 shows CE in the mixed SOA/squalane particles as a function of squalane mass fraction, where CE is calculated by eq 1 using LSSP data. CE increases with increasing squalane mass fraction due to its liquid phase. The accompanying cartoons indicate what a core−shell morphology would hypothetically look like if layering followed the same order in which the mixed-particles were prepared and without any morphological rearrangement. The numbers refer to each of the three stages of the experiment: (1) seed particles only, (2) seed particles with the condensed coating layer, and (3) the particles after heating. Regardless of the ordering in which these mixed-particles were formed, CE can be parametrized as a function of squalane mass fraction by the following equation

$$\mathrm{CE} = 0.21 + 1.5\chi_{sq} + -0.73\chi_{sq}^2 \quad (3)$$

where χ_{sq} is the squalane mass fraction calculated from eq 2.

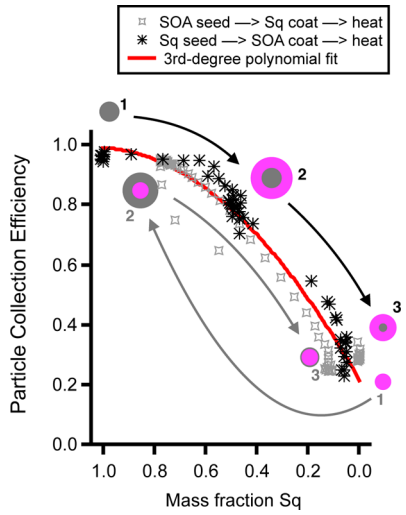

Figure 4. Particle CE as a function of overall squalane mass % for mixed-particle experiments followed by a heating ramp, prepared in two different ways: SOA seeds with squalane condensation (gray), and squalane seeds with SOA condensation (black). Cartoons illustrate what particles would look like if morphology is core−shell and follows the preparation sequence without any rearrangement of the two phases (where pink represents SOA and gray represents squalane). Numbers demarcate each stage of the experiment: (1) seed particles only, (2) mixed-particles, (3) mixed-particles after heating.

Researchers often assume that coating experiments produce particles with the second constituent forming a shell around a core made up of the first constituent. However, for two-phase systems there is likely only one minimum free energy morphology. Given that CE can be described solely as a function of squalane mass fraction, it is possible that a morphological reordering may have occurred in either or both experiments, and that the sampled particles have the same morphology regardless of the preparation order. On the other hand, particle bounce is a complex phenomenon governed by kinetic energy transfer from particle to vaporizer, and both the phase state of the particle surface and of the core are likely important. Thus, we can draw no definitive conclusions about morphology from these data, though this plot separately highlights the need to understand CE in situations where the phase-state of particles is dynamic over the course of a measurement period.

Comparative Volatility Analysis of Mixed-Particles. Figure 5 illustrates the process of using the CE parametrization in order to correct our data to estimate the SOA mass fraction remaining (MFR) after the smog chamber is heated. The top panel shows the calculated CE to be used for all organic mass in the AMS, along with the smog chamber temperature. Panel two shows the uncorrected and CE-corrected m/z 43 mass (a tracer for SOA in this system). After applying the CE correction (which simply means dividing the mass signal by the CE value for a given data point), a first-order exponential wall loss curve is fit to m/z 43 to find the particle wall-loss constant for the time-period after SOA formation and prior to heating. In Figure 5c, MFR is plotted for SOA using m/z 43 as a tracer with and without correcting for changing CE. MFR for SOA is calculated as follows:

$$\mathrm{MFR}_{\mathrm{SOA}} = \frac{m/z43}{m/z43_{\mathrm{fit}}} \quad (4)$$

DOI: 10.1021/acs.est.5b01692
Environ. Sci. Technol. 2015, 49, 9724−9732

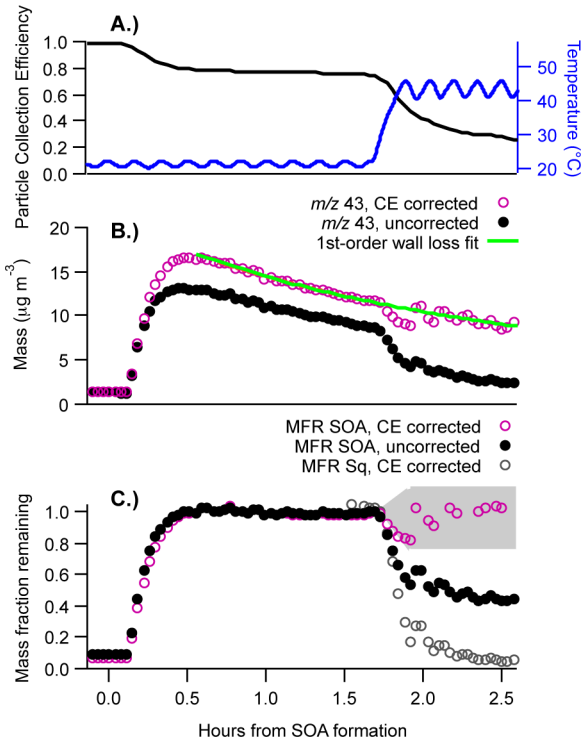

Figure 5. Time series illustrating calculation of SOA mass fraction remaining (MFR) after smog chamber heating from 22 to 44 °C for same experiment shown in Figure 2. In top panel (A.), particle CE is parametrized according to the fitted equation from Figure 4. The uncorrected and CE-corrected m/z 43 masses are shown in the middle panel (B.), along with the first-order exponential fit used to extrapolate the mass if there were no heating. In the bottom panel (C.), the SOA MFR is calculated by dividing the measured mass with the wall loss fitted mass, shown in the bottom panel. These corrections are necessary to estimate the MFR of SOA after heating because we know that CE is variable throughout this experiment. There is no substantial decrease in SOA MFR after applying the CE correction, though there is substantial uncertainty (gray band) in this calculation due to fluctuations in mass signal with temperature.

where the corrected m/z 43 is normalized by the extrapolated mass based on our wall-loss fit (m/z 43_{fit}). This approach of estimating MFR_{SOA} requires two assumptions. First, we assume that the mass of m/z 43 decays according to first-order wall loss (e.g., Tkacik et al.[33]), and would continue to do so as extrapolated without any heating. Second, we assume that m/z 43 is a perfect tracer for all components of the SOA over the entire temperature range explored here. Previous work has shown that the fraction of m/z 43 for "pure" SOA from α-pinene + O_3 (f_{43}) decreases upon heating,[34] meaning that at higher temperatures the OA is relatively enriched in molecules that contribute less to the m/z 43 fragment than at the reference temperature. This would mean that our MFR measurements for SOA would be biased low, as m/z 43 might underrepresent the total amount of SOA. Based on thermally denuded SOA measurements by Lambe et al.[34] (see Supporting Information Figure S5 of Lambe et al.), there is a very minimal decrease in f_{43} at temperatures similar to those in our smog chamber heat ramp (between 0 and 15% for MFR decrease from 1 to 0.5), we anticipate this bias to contribute at most 15% error to the SOA MFR.

We calculate the SOA MFR to be $\approx 1 \pm 0.2$ in all of these mixed-particle experiments. There are clear fluctuations in mass signals upon heating that align directly with the temperature fluctuations, and may be attributable to thermally driven, spatial concentration gradients within the chamber causing inhomogeneities in our measurements. We have indicated this uncertainty (gray shaded band) on Figure 4. On the other hand, approximately 90% of the squalane evaporates within an hour of heating. This comparative volatility analysis allows us to conclude that the majority of the suspended SOA in these experiments is comprised of compounds less volatile than squalane.

DISCUSSION

We have shown that when one sequentially prepares two-phase squalane/SOA particles and heats them in a smog chamber, squalane significantly, and preferentially, evaporates. This is illustrated by a bulk measurement of the mass fraction of squalane, but further supported by size-resolved mass distributions of marker mass spectral fragments and mass signals from individual particles.

The morphology of these particles has important implications for the larger findings of this work. Vaden et al.[35] provide evidence for core−shell morphology in mixed particles prepared from hydrophobic, nonpolar seed particles serving as surface area for SOA condensation. Using single-particle laser-ablation mass spectrometry, they report a core−shell morphology for SOA-coated DOP in which the SOA remains on the outside of the DOP core for the duration of their experiment (multiple hours). Additionally, they report an adsorbed monolayer of DOP on the outside of the SOA shell. Based on the results of Vaden et al., we expect our particles to be core−shell with SOA on the outside when we prepare SOA in the presence of squalane seeds, with the possibility of an adsorbed squalane layer outside of the SOA shell.

In our mixed-particle experiments, the majority (~90%) of the squalane mass rapidly evaporates into the gas-phase upon heating, while almost all of the SOA mass remains. Thus, if the morphology of these particles is core−shell with SOA on the outside, then there are minimal diffusive limitations to the evaporation of squalane through the SOA layer at this elevated temperature. The majority of squalane mass would be moving, on the order of tens of minutes, through a substantial SOA coating (e.g., ~30 nm thick SOA shell for a particle with a 250 nm diameter). This finding would be in disagreement with a number of recent studies that make a case for organic diffusion coefficients in SOA being so low that equilibration might not be possible on atmospheric time scales.[5,13,14] While there is a possibility of a substantial amount of squalane adsorbed onto the surface of the SOA shell (Vaden et al.[35] report a 4 nm adsorbed layer on 158 nm particles, comprising 12% of the particle mass), this would not change the overall conclusion here. For a given mass fraction of squalane in a particle, shifting some of the squalane mass to an outer layer increases the thickness of the SOA shell. And given that we see squalane MFR decreasing from 1 to near-zero during the heat ramp, even with the possibility of a substantial outer layer, the large majority of squalane would be moving through the SOA shell.

We should consider other possible morphologies, however, as our measurements do not directly diagnose morphology. If, on the other hand, the SOA trades places with the squalane and the SOA forms the core, or if the morphology is partially engulfed (as concluded by Cappa and Wilson[31] for LO-SOA mixed-particles), then our data do not constrain organic diffusivity within the condensed SOA phase. In either of

DOI: 10.1021/acs.est.5b01692
Environ. Sci. Technol. 2015, 49, 9724−9732

these cases, squalane would have an interface with air, and evaporation could simply proceed through this "window." However, this is unexpected given the results of Vaden et al.,[35] and would call into question the common assumption that the second material condensed necessarily forms a "coating" or shell.

Nonetheless, there does exist a single, lowest-energy configuration for two immiscible, condensed phases combined in a droplet suspended in air. A theoretical means of predicting this equilibrium morphology is provided by Reid et al.,[36] but requires knowing all interfacial energies in the system. While the surface tension of squalane is known (26 mN m^{-1})[37] and very similar to that of DOP used in the Vaden et al.[35] study, neither the SOA surface tension nor the SOA−squalane interfacial tensions are known, removing the possibility of predicting the equilibrium morphology. However, if a metastable morphology is initially formed (e.g., an SOA shell on a squalane core), though some other configuration is more energetically favorable (e.g., squalane shell, SOA core), it is conceivable that the shift to the stable configuration still might not occur for two reasons: (1) if some nonspherical geometry must be adopted to make the shift, then the energy required to reach the more stable state could make the shift unfavorable, and (2) the kinetics of such a rearrangement, even if energetically favorable, would likely be slow if SOA has a high viscosity, as has been reported recently.[7,38]

Regardless of morphological concerns, these experiments allow us to assess the volatility of our SOA relative to that of a calibration compound with known volatility, in this case squalane. Because we see almost all of the squalane evaporate by the end of the heating period (MFR_{Sq} = 0.05) compared to almost none of the SOA ($MFR_{SOA} \sim 1$), we conclude that to first order most of the suspended SOA is made of components less volatile than squalane. However, in some studies α-pinene SOA begins to evaporate in 30s residence time thermodenuders at roughly 50 °C and almost completely vanishes between 75 to 100 °C (e.g., Lee et al.,[39] Asa-Awuku et al.[10]), suggesting that either evaporation or thermal decomposition occurs just above the temperature we could reach in our smog chamber, though in other studies (e.g., Cappa and Wilson et al.[31]), α-pinene SOA evaporates at much higher temperatures. Our data suggest that the slow SOA evaporation under vapor-free conditions observed in, for example, Vaden et al.[12] may simply be due to the low-volatility nature of SOA from α-pinene + O_3 and not due to diffusion limitations.

The mass loss of squalane in these experiments is perhaps surprising, given its relatively low volatility ($C^{sat} = 8 \times 10^{-2}$ μg m^{-3} at T = 25 °C). Were the squalane evaporating solely to achieve its new saturation concentration at the elevated temperature (C^{sat} = 1.2 μg m^{-3} at T = 44 °C) (estimated using SIMPOL[28]), the mass loss would be on the order of 1 μg m^{-3}, which is much less than what we see in these experiments. Thus, we believe that the evaporative driving force is the result of absorption of squalane vapors by the Teflon walls of the smog chamber. It is possible but unlikely that squalane is preferentially lost to the Teflon walls. In a previous study, Matsunaga and Ziemann showed that oxidized organics are somewhat more absorptive in Teflon than reduced organics of similar volatility.[21]

In summary, we find that studying the evaporation of mixed-particles has the potential to directly probe the diffusivity of SOA, though knowledge of particle morphology is crucial. Additionally, evaporation studies of mixed-particles can be used to constrain the fraction of a multicomponent material (SOA in this case) with lower volatility than a pure-component material with known vapor pressure. We find that, to first order, the large majority of the SOA from α-pinene + O_3 has a volatility lower than that of squalane, and this comparative volatility analysis could be extended to other systems. We also provide further evidence that supports previous work showing that nonpolar, hydrophobic pure-component OA and SOA from α-pinene + O_3 form separate phases.[9,35] However, atmospheric POA (e.g., diesel exhaust) does have some polarity even prior to atmospheric oxidation,[10] and thus POA surrogates like squalane may not necessarily reflect mixing behavior in the real atmosphere. This work demonstrates that more studies on OA phase state and morphology are critical to fill our current gaps in knowledge of organic aerosol transformation in the atmosphere.

■ ASSOCIATED CONTENT

Supporting Information

Time series of squalane MFR, squalane mass, and SOA mass for all mixed-particle experiments performed are presented. A representative mixed-particle experiment where squalane was condensed onto SOA seed particles is presented. Lastly, shell thickness versus particle size plots are shown. The Supporting Information is available free of charge on the ACS Publications website at DOI: 10.1021/acs.est.5b01692.

■ AUTHOR INFORMATION

Corresponding Author

*Phone: (412) 268-4415; e-mail: nmd@cmu.edu.

Notes

The authors declare no competing financial interest.

■ ACKNOWLEDGMENTS

This research was supported by grant CHE1012293 from the National Science Foundation. The High-Resolution Aerosol Mass Spectrometer was purchased with Major Research Instrumentation funds from NSF CBET0922643 and the Wallace Research Foundation.

■ REFERENCES

(1) IPCC. *Climate Change 2013: The Physical Science Basis. Contribution of Working Group I to the Fifth Assessment Report of the Intergovernmental Panel on Climate Change*; Stocker, T., Qin, D., Plattner, G.-K., Tignor, M., Allen, S., Boschung, J., Nauels, A., Xia, Y., Bex, V., Midgley, P., Eds.; Cambridge University Press: Cambridge, United Kingdom, 2013; Chapter Technical Summary.

(2) Jimenez, J. L.; et al. Evolution of Organic Aerosols in the Atmosphere. *Science* **2009**, *326*, 1525−1529.

(3) Volkamer, R.; Jimenez, J. L.; San Martini, F.; Dzepina, K.; Zhang, Q.; Salcedo, D.; Molina, L. T.; Worsnop, D. R.; Molina, M. J. Secondary organic aerosol formation from anthropogenic air pollution: Rapid and higher than expected. *Geophys. Res. Lett.* **2006**, *33*, L17811.

(4) Strader, R.; Lurmann, F.; Pandis, S. N. Evaluation of secondary organic aerosol formation in winter. *Atmos. Environ.* **1999**, *33*, 4849−4863.

(5) Abramson, E.; Imre, D.; Beránek, J.; Wilson, J.; Zelenyuk, A. Experimental determination of chemical diffusion within secondary organic aerosol particles. *Phys. Chem. Chem. Phys.* **2013**, *15*, 2983−2991.

(6) Shrivastava, M.; Zelenyuk, A.; Imre, D.; Easter, R.; Beránek, J.; Zaveri, R. A.; Fast, J. Implications of low volatility SOA and gas-phase fragmentation reactions on SOA loadings and their spatial and

DOI: 10.1021/acs.est.5b01692
Environ. Sci. Technol. 2015, 49, 9724−9732

temporal evolution in the atmosphere. *J. Geophys. Res.* **2013**, *118*, 3328−3342.
(7) Kidd, C.; Perraud, V.; Wingen, L. M.; Finlayson-Pitts, B. J. Integrating phase and composition of secondary organic aerosol from the ozonolysis of α-pinene. *Proc. Natl. Acad. Sci. U. S. A.* **2014**, *111*, 7552−7557.
(8) Bowman, F. M.; Eskelson, K. Thermodynamic consistency of Raoult's Law and Henry's Law approaches for multiphase organic aerosol partitioning. *J. Atmos. Chem.* **2009**, *64*, 179−193.
(9) Song, C.; Zaveri, R. A.; Alexander, M. L.; Thornton, J. A.; Madronich, S.; Ortega, J. V.; Zelenyuk, A.; Yu, X.-Y.; Laskin, A.; Maughan, D. A. Effect of hydrophobic primary organic aerosols on secondary organic aerosol formation from ozonolysis of alpha-pinene. *Geophys. Res. Lett.* **2007**, *34*, L20803.
(10) Asa-Awuku, A.; Miracolo, M. A.; Kroll, J. H.; Robinson, A. L.; Donahue, N. M. Mixing and phase partitioning of primary and secondary organic aerosols. *Geo. Res. Lett.* **2009**, *36*, L15827.
(11) Robinson, E. S.; Saleh, R.; Donahue, N. M. Organic Aerosol Mixing Observed by Single-Particle Mass Spectrometry. *J. Phys. Chem. A* **2013**, *117*, 13935−13945.
(12) Vaden, T.; Imre, D.; Beránek, J.; Shrivastava, M.; Zelenyuk, A. Evaporation kinetics and phase of laboratory and ambient secondary organic aerosol. *Proc. Natl. Acad. Sci. U. S. A.* **2011**, *108*, 2190−2195.
(13) Perraud, V.; Bruns, E.; Ezell, M.; Johnson, S.; Yu, Y.; Alexander, M.; Zelenyuk, A.; Imre, D.; Chang, W.; Dabdub, D. Nonequilibrium atmospheric secondary organic aerosol formation and growth. *Proc. Natl. Acad. Sci. U. S. A.* **2012**, *109*, 2836−2841.
(14) Zelenyuk, A.; Imre, D.; Beránek, J.; Abramson, E.; Wilson, J.; Shrivastava, M. Synergy between Secondary Organic Aerosols and Long-Range Transport of Polycyclic Aromatic Hydrocarbons. *Environ. Sci. Technol.* **2012**, *46*, 12459−12466.
(15) Ehn, M.; et al. A large source of low-volatility secondary organic aerosol. *Nature* **2015**, *506*, 476−479.
(16) Kokkola, H.; Yli-Pirilä, P.; Vesterinen, M.; Korhonen, H.; Keskinen, H.; Romakkaniemi, S.; Hao, L.; Kortelainen, A.; Joutsensaari, J.; Worsnop, D. R.; Virtanen, A.; Lehtinen, K. E. J. The role of low volatile organics on secondary organic aerosol formation. *Atmos. Chem. Phys.* **2014**, *14*, 1689−1700.
(17) Pathak, R. K.; PResto, A. A.; Lane, T. E.; Stanier, C. O.; Donahue, N. M.; Pandis, S. N. Ozonolysis of α-pinene: parameterization of secondary organic aerosol mass fraction. *Atmos. Chem. Phys.* **2007**, *7*, 3811−3821.
(18) Saleh, R.; Donahue, N. M.; Robinson, A. L. Time Scales for Gas-Particle Partitioning Equilibration of Secondary Organic Aerosol Formed from Alpha-Pinene Ozonolysis. *Environ. Sci. Technol.* **2013**, *47*, 5588−5594.
(19) Loza, C. L.; Coggon, M. M.; Nguyen, T. B.; Zuend, A.; Flagan, R. C.; Seinfeld, J. H. On the Mixing and Evaporation of Secondary Organic Aerosol Components. *Environ. Sci. Technol.* **2013**, *47*, 6173−6180.
(20) Renbaum-Wolff, L.; Grayson, J. W.; Bertram, A. K. Technical Note: New methodology for measuring viscosities in small volumes characteristic of environmental chamber particle samples. *Atmos. Chem. Phys.* **2013**, *13*, 791−802.
(21) Matsunaga, A.; Ziemann, P. J. Gas-Wall Partitioning of Organic Compounds in a Teflon Film Chamber and Potential Effects on Reaction Product and Aerosol Yield Measurements. *Aerosol Sci. Technol.* **2010**, *44*, 881−892.
(22) DeCarlo, P. F.; Kimmel, J. R.; Trimborn, A.; Northway, M. J.; Jayne, J. T.; Aiken, A. C.; Gonin, M.; Fuhrer, K.; Horvath, T.; Docherty, K. S.; Worsnop, D. R.; Jimenez, J. L. Field-Deployable, High-Resolution, Time-of-Flight Aerosol Mass Spectrometer. *Anal. Chem.* **2006**, *78*, 8281−8289.
(23) Cross, E.; Onasch, T.; Canagaratna, M.; Jayne, J.; Kimmel, J.; Yu, X.; Alexander, M.; Worsnop, D.; davidovits, P. Single particle characterization using a light scattering module coupled to a time-of-flight aerosol mass spectrometer. *Atmos. Chem. Phys.* **2009**, *9*, 7769−7793.
(24) Docherty, K. S.; Jaoui, M.; Corse, E.; Jimenez, J. L.; Offenberg, J. H.; Lewandowski, M.; Kleindienst, T. E. Collection Efficiency of the Aerosol Mass Spectrometer for Chamber-Generated Secondary Organic Aerosols. *Aerosol Sci. Technol.* **2013**, *47*, 294−309.
(25) Huffman, J. A.; Jayne, J. T.; Drewnick, F.; Aiken, A. C.; Onasch, T.; Worsnop, D. R.; Jimenez, J. L. Design, Modeling, Optimization, and Experimental Tests of a Particle Beam Width Probe for the Aerodyne Aerosol Mass Spectrometer. *Aerosol Sci. Technol.* **2005**, *39*, 1143−1163.
(26) Liu, S.; Russell, L. M.; Sueper, D. T.; Onasch, T. B. Organic particle types by single-particle measurements using a time-of-flight aerosol mass spectrometer coupled with a light scattering module. *Atmos. Meas. Tech.* **2013**, *6*, 187−197.
(27) Ulbrich, I. M.; Canagaratna, M. R.; Zhang, Q.; Worsnop, D. R.; Jimenez, J. L. Interpretation of organic components from Positive Matrix Factorization of aerosol mass spectrometric data. *Atmos. Chem. Phys.* **2009**, *9*, 2891−2918.
(28) Pankow, J.; Asher, W. SIMPOL. 1: a simple group contribution method for predicting vapor pressures and enthalpies of vaporization of multifunctional organic compounds. *Atmos. Chem. Phys.* **2008**, *8*, 2773−2796.
(29) Donahue, N. M.; Robinson, A. L.; Trump, E. R.; Riipinen, I.; Kroll, J. H. Volatility and Aging of Atmospheric Organic Aerosol. *Top. Curr. Chem.* **2012**, *339*, 97−143.
(30) Robinson, E. S., Donahue, N. M. Collection efficiency of a-pinene secondary organic aerosol particles explored via light scattering single particle aerosol mass spectrometry *Atmos. Meas. Tech. Discuss.* to be submitted.
(31) Cappa, C. D.; Wilson, K. R. Evolution of organic aerosol mass spectra upon heating: implications for OA phase and partitioning behavior. *Atmos. Chem. Phys.* **2011**, *11*, 1895−1911.
(32) Alfarra, M. R. *Insights Into Atmospheric Organic Aerosols Using an Aerosol Mass Spectrometer*. Ph.D. thesis, University of Manchester, 2004.
(33) Tkacik, D. S.; Presto, A. A.; Donahue, N. M.; Robinson, A. L. Secondary Organic Aerosol Formation from Intermediate-Volatility Organic Compounds: Cyclic, Linear, and Branched Alkanes. *Environ. Sci. Technol.* **2012**, *46*, 8773−8781.
(34) Lambe, A. T.; Onasch, T. B.; Massoli, P.; Croasdale, D. R.; Wright, J. P.; Ahern, A. T.; Williams, L. R.; Worsnop, D. R.; Brune, W. H.; davidovits, P. Laboratory studies of the chemical composition and cloud condensation nuclei (CCN) activity of secondary organic aerosol (SOA) and oxidized primary organic aerosol (OPOA). *Atmos. Chem. Phys.* **2011**, *11*, 8913−8928.
(35) Vaden, T.; Song, C.; Zaveri, R. A.; Imre, D.; Zelenyuk, A. Atmospheric Chemistry Special Feature: Morphology of mixed primary and secondary organic particles and the adsorption of spectator organic gases during aerosol formation. *Proc. Natl. Acad. Sci. U. S. A.* **2010**, *107*, 6658−6663.
(36) Reid, J. P.; Dennis-Smither, B. J.; Kwamena, N.-O. A.; Miles, R. E. H.; Hanford, K. L.; Homer, C. J. The morphology of aerosol particles consisting of hydrophobic and hydrophilic phases: hydrocarbons, alcohols and fatty acids as the hydrophobic component. *Phys. Chem. Chem. Phys.* **2011**, *13*, 15559−15572.
(37) Lafosse, M.; Dreux, M. Étude du mélange binaire squalane-stéaronitrile comme phase stationnaire: I. Comparaison des résultats provenant d'une étude par chromatographie en phase gazeuse avec ceux résultant des mesures de tension superficielle. *J. Chromatogr. A* **1980**, *188*, 315−322.
(38) Renbaum-Wolff, L.; Grayson, J. W.; Bateman, A. P.; Kuwata, M.; Sellier, M.; Murray, B. J.; Shilling, J. E.; Martin, S. T.; Bertram, A. K. Viscosity of alpha-pinene secondary organic material and implications for particle growth and reactivity. *Proc. Natl. Acad. Sci. U. S. A.* **2013**, *110*, 8014−8019.
(39) Lee, B.-H.; Pierce, J. R.; Engelhart, G. J.; Pandis, S. N. Volatility of secondary organic aerosol from the ozonolysis of monoterpenes. *Atmos. Environ.* **2011**, *45*, 2443−2452.

DOI: 10.1021/acs.est.5b01692
Environ. Sci. Technol. 2015, 49, 9724−9732